Table 1 Performance of trajectories

No.	Description	t_1-t_0	P_{11}	P_{22}	P_{33}	ϕ	
						$a_1 = 0.167$	$a_1 = 10$
1	Nominal; all measurements	200.0	796.1	5.2	8.3	603.5	24768.3
2	Optimal for $a_1 = 0.167$; all measurements	200.46	787.2	5.0	8.6	601.5	...
3	Optimal for $a_1 = 10$; all measurements	200.69	785.0	5.0	8.7	...	24634.9
4	Nominal; measure y	200.0	1110	7.3	159.2	580.5	...
5	Optimal for $a_1 = 0.167$; measure y	201.67	1098	6.9	159.7	569.4	...

The fixed terms are a guess at the effect of the surface roughness directly below the vehicle. The noise in the control system was assumed to have $\sigma_b^2 = 0.64$ ft^2-sec^{-4} and $\sigma_\theta^2 = 10^{-4}$.

The effect of the weights given to the uncertainty terms was found by assuming them to be in the arbitrary ratio 1:160:100 and scaling them up or down together. Some results with the full set of measurements are shown as trajectories 1, 2, and 3 in Table 1. Note the small changes in the variances. The steering programs are shown in Fig. 2.

The effects of simpler measuring equipment were found by assuming σ_u and σ_v to be infinite, leaving only the measurement of altitude. In addition, the weight given to the variance of horizontal velocity was set equal to zero, since, in the parallel field, with only y being measured, there is no way to infer the horizontal velocity from the measurements. The results of this are in Table 1 as trajectories 4 and 5, and the steering programs are shown in Fig. 2.

The values of a_i used in the foregoing are arbitrary. To talk in terms of overall optimization, one must find values of a_i which correctly represent the trade-off between uncertainty and propellant during the final descent phase. Consider

$$m = m(t_1 - t_0, P_{11})$$

from which

$$\Delta m/\dot{m} = \Delta t_1 + (1/\dot{m})(\partial m/\partial P_{11})\Delta P_{11}$$

This is the same as $\Delta\phi$ if one neglects P_{22} and P_{33} and sets

$$a_1 = (1/\dot{m})(\partial m/\partial P_{11})$$

Now, if the vehicle makes its final descent from $y = 3(P_{11})^{1/2}$ at velocity v_d,

$$\Delta m_d = \dot{m}_d\, t_d = \dot{m}_d[3(P_{11})^{1/2}/v_d]$$

Thus

$$\partial m/\partial P_{11} = 3\dot{m}_d/2v_d(P_{11})^{1/2}$$

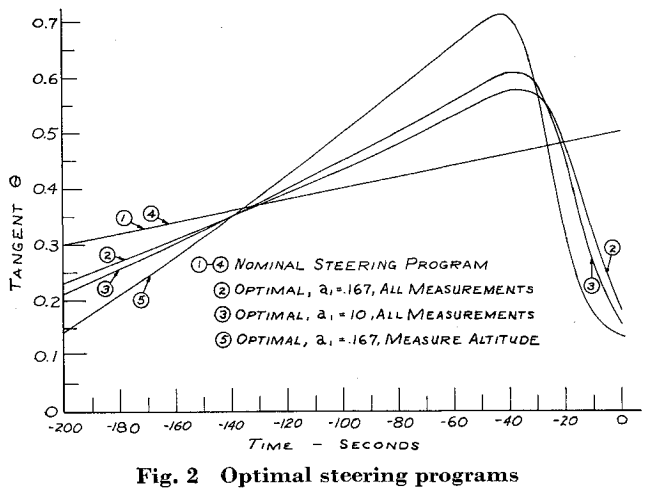

Fig. 2 Optimal steering programs

or

$$a_1 = (\dot{m}_d/\dot{m})[3/2v_d(P_{11})^{1/2}]$$

From the nominal trajectory, $P_{11} = 787$, $\dot{m}_d/\dot{m} = \frac{1}{12}$, and with $v_d = 10$ fps, $a_1 \cong 0.00045$.

Thus, for this example, unless the noise level is considerably larger than assumed here, the inclusion of the statistics is unimportant. However, the technique has been shown here to be feasible and is now available for more sensitive situations, such as atmospheric entry.

References

[1] Garfinkel, B., "Minimal problems in airplane performance," Quart. Appl. Math. IX, 149–162 (1951).

[2] Leitmann, G., "On a class of variational problems in rocket flight," J. Aerospace Sci. **26**, 586–591 (1959).

[3] Bryson, A. E. and Denham, W., "A steepest ascent method for solving optimum programming problems," Rept. BR-1303, Missile and Space Div., Raytheon Co., Bedford, Mass. (August 1961).

[4] Bryson, A. E. and Denham, W., "Multivariable terminal control for minimum mean square deviation from a nominal path," Rept. BR-1333, Missile and Space Div., Raytheon Co., Bedford, Mass. (September 1961).

[5] Kelley, H. J., "Guidance theory and extremal fields, Inst. Radio Engrs. Natl. Aero-Space Electronics Conference, Dayton, Ohio (May 1962); also Inst. Radio Engrs. Trans. Auto. Control **AC-7**, 75–81 (October 1962).

[6] Kalman, R. E. and Bucy, R. S., "New results in linear filtering and prediction theory," J. Basic Eng., Trans. Am. Soc. Mech. Engrs. (1960); also Am. Soc. Mech. Engrs. Paper 60-JAC-12 (1960).

[7] Berman, L. J., "Optimum soft landing trajectories," Air Force Office Sci. Research 519, Mass. Inst. Tech., Part I: "Analysis" (March 1961); Part II: "Numerical results" (March 1962).

[8] Steinker, G. E., "Solutions for optimal stochastic trajectories," S.M. thesis, Mass. Inst. Tech. (January 1963).

Cross-Thermoelastic Phenomenon in Heterogeneous Aeolotropic Plates

YEHUDA STAVSKY*
Israel Institute of Technology, Technion City, Israel

THIS note is concerned with the thermoelastic stress-strain relations in a heterogeneous aeolotropic plate theory that is based on the Euler-Bernoulli hypothesis.

Consider a thin elastic plate of constant thickness h which is heterogeneous in the thickness direction z. Let x, y be the

Received by IAS August 22, 1962; revision received September 10, 1962.

* Senior Lecturer, Department of Mechanics.

coordinates in the undeflected bottom face of the plate ($z = 0$). Assume the temperature distributions throughout the plate to be prescribed and independent of the deformation of the system. Denoting by e_{ij} the elastic compliance moduli and α_i the coefficients of thermal expansion of the medium, one can write the following thermal stress-strain relations:

$$\begin{bmatrix} \epsilon_x \\ \epsilon_y \\ \epsilon_{xy} \end{bmatrix} = \begin{bmatrix} e_{xx} & e_{xy} & e_{xs} & \alpha_x \\ e_{yx} & e_{yy} & e_{ys} & \alpha_y \\ e_{sx} & e_{sy} & e_{ss} & \alpha_s \end{bmatrix} \begin{bmatrix} \tau_x \\ \tau_y \\ \tau_{xy} \\ T \end{bmatrix} \tag{1}$$

Assume the symmetry relations $e_{xy} = e_{yx}$, $e_{xs} = e_{sx}$, $e_{ys} = e_{sy}$, and, furthermore, that

$$e_{xx} = e_{xx}(z) \text{ etc.} \tag{2}$$

$$\alpha_x = \alpha_x(z) \text{ etc.} \tag{3}$$

where T denotes the change in temperature from the initial, stress-free state, being a function of both the space and time coordinates

$$T = T(x,y,z,t) \tag{4}$$

Following Timoshenko and Goodier's terminology,[1] ϵ_x, ϵ_y, ϵ_{xy} are named the actual strain components, and

$$\epsilon_x^* = \epsilon_x - \alpha_x T \text{ etc.} \tag{5}$$

is the strain part due to stress. Using Eqs. (5), Eqs. (1) are rewritten to read

$$[\epsilon^*] = [e][\tau] \tag{6}$$

Inverting Eqs. (6), one obtains

$$\begin{bmatrix} \tau_x \\ \tau_y \\ \tau_{xy} \end{bmatrix} = \begin{bmatrix} E_{xx} & E_{xy} & E_{xs} & \mathbf{A}_x \\ E_{yx} & E_{yy} & E_{ys} & \mathbf{A}_y \\ E_{sx} & E_{sy} & E_{ss} & \mathbf{A}_s \end{bmatrix} \begin{bmatrix} \epsilon_x \\ \epsilon_y \\ \epsilon_{xy} \\ T \end{bmatrix} \tag{7}$$

where

$$-[\mathbf{A}] = [E][\alpha] \tag{8}$$

Introducing

$$\tau_x^* = \tau_x - \mathbf{A}_x T \qquad \tau_y^* = \tau_y - \mathbf{A}_y T$$
$$\tau_{xy}^* = \tau_{xy} - \mathbf{A}_{xy} T \tag{9}$$

Equations (7) are rewritten as follows:

$$[\tau^*] = [E][\epsilon] \tag{10}$$

Defining reference surface strains (at $z = 0$) and bending curvatures, as in usual in plate theory, the following strain-displacement relations of linear plate theory, based on the Euler-Bernoulli hypothesis, are possible:

$$\epsilon_x = \epsilon_x^0 + z\kappa_x \qquad \epsilon_y = \epsilon_y^0 + z\kappa_y$$
$$\epsilon_{xy} = \epsilon_{xy}^0 + z\kappa_{xy} \tag{11}$$

$$\epsilon_x^0 = u_{,x} \qquad \epsilon_y^0 = v_{,y} \qquad \epsilon_{xy}^0 = u_{,y} + v_{,x} \tag{12}$$

$$\kappa_x = -w_{,xx} \qquad \kappa_y = -w_{,yy} \qquad \kappa_{xy} = -2w_{,xy} \tag{13}$$

Introduction of Eqs. (7) into the definitions

$$N_x = \int_0^h \tau_x dz \qquad M_x = \int_0^h \tau_x z dz \tag{14}$$

and so on, for resultants and couples, gives a system of thermal stress-strain relations

$$\begin{bmatrix} N^* \\ M^* \end{bmatrix} = \left[\begin{array}{c|c} A & B \\ \hline B & D \end{array}\right] \begin{bmatrix} \epsilon^0 \\ \kappa \end{bmatrix} \tag{15}$$

The elastic areas, the elastic statical moments, and the elastic moments of inertia are given, correspondingly, by

$$(A_{xx}, B_{xx}, D_{xx}) = \int_0^h (1, z, z^2) E_{xx} dz, \text{ etc.} \tag{16}$$

The starred resultants and couples are defined as follows:

$$N_x^* = N_x - N_{xt} \qquad N_y^* = N_y - N_{yt}$$
$$N_{xy}^* = N_{xy} - N_{st} \tag{17}$$

$$M_x^* = M_x - M_{xt} \qquad M_y^* = M_y - M_{yt}$$
$$M_{xy}^* = M_{xy} - M_{st} \tag{18}$$

where the quantities N_{xt}, M_{xt} are given by

$$(N_{xt}, M_{xt}) = \int_0^h (1, z)\mathbf{A}_x T dz, \text{ etc.} \tag{19}$$

Inverting the system (15) the reference surface strain components and the plate curvatures are obtained in terms of the starred resultants and couple

$$\begin{bmatrix} \epsilon^0 \\ \kappa \end{bmatrix} = \left[\begin{array}{c|c} a & b \\ \hline c & d \end{array}\right] \begin{bmatrix} N^* \\ M^* \end{bmatrix} \tag{20}$$

in which a, b, c, d are 3×3 matrices related to the symmetric matrices A, B, D by the following relations:

$$[a] = [A^{-1}] + [X][Z^{-1}][Y] \tag{21}$$

$$[b] = -[X][Z^{-1}] = [c]^T \tag{22}$$

$$[c] = -[Z^{-1}][Y] \tag{23}$$

$$[d] = [Z^{-1}] \tag{24}$$

where

$$[X] = [A^{-1}][B] \tag{25}$$

$$[Y] = [B][A^{-1}] \tag{26}$$

$$[Z] = [D] - [Y][B] \tag{27}$$

Note that A, B, D, a, d are symmetric matrices but that b, c are, generally, not symmetric matrices.

Introducing Eqs. (11–13) in Eqs. (10) and using Eqs. (20), one finds the following expressions for the stress components in terms of stress resultants and couples:

$$[\tau^*] = [E]\{([a] + z[c])[N^*] + ([b] + z[d])[M^*]\} \tag{28}$$

These expressions clearly show a cross-thermoelasticity effect: namely, *each* stress component is a linear function of *all* stress resultants and couples as well as of *all* the quantities N_{it}, M_{it}.

Equations (28) may be considered as an extension of Eqs. (70) in Ref. 2 for the isothermal plate to the thermoelastic plate.

Since there is a complete analogy between these two equations, one can deduce the same special classes of heterogeneity for which the cross phenomenon vanishes.[2] Such a special case, for which all elastic moduli (Young's modulus E and Poisson's ratio ν) have the same variation through the plate thickness, was given recently by Newman and Forray.[3]

Note that present results hold also for a nonlinear plate theory that accounts for finite deflections. One then only has to replace Eqs. (13) by

$$\epsilon_x^0 = u_{,x} + \tfrac{1}{2}w_{,x}^2 \qquad \epsilon_y^0 = v_{,y} + \tfrac{1}{2}w_{,y}$$
$$\epsilon_{xy}^0 = u_{,y} + v_{,x} + w_{,x}w_{,y} \tag{29}$$

and all other equations remain unaltered, including the main result (28).

References

[1] Timoshenko, S. and Goodier, J. N., *Theory of Elasticity* (McGraw-Hill Book Co. Inc., New York, 1951), 2nd ed., p. 406.

[2] Stavsky, Y., "Bending and stretching of laminated aeolotropic plates," Proc. Am. Soc. Civ. Engrs., J. Eng. Mech. Div. 87, 31–56 (1961).
[3] Newman, M. and Forray, M., "Thermal stresses and deflections in thin plates with temperature-dependent elastic moduli," J. Aerospace Sci. 29, 372–373 (1962).

Simplification of the Shock-Tube Equation

J. Gordon Hall* and Anthony L. Russo†

Cornell Aeronautical Laboratory Inc., Buffalo, N. Y.

A useful simplification of the shock-tube equation is pointed out for shock Mach numbers exceeding about 3. For given driver gas specific heat ratio, shock-tube performance can be expressed explicitly for all initial conditions (including area change) by a single curve. The two basic variables are the shock strength normalized in terms of diaphragm pressure ratio, and the diaphragm density ratio. Universal performance curves are given in this form. Application to tailored-interface conditions and optimum performance of buffered tubes is described.

THE ideal-gas shock-tube equation in terms of shock Mach number M_s and initial conditions before diaphragm rupture is[1]

$$\frac{1}{gP_{41}}\left[\frac{2\gamma_1}{\gamma_1+1}M_s^2-\frac{\gamma_1-1}{\gamma_1+1}\right]=\left[1-\frac{(\gamma_4-1)(M_s^2-1)}{(\gamma_1+1)A_{41}M_s}g^{-(\gamma_4-1)/2\gamma_4}\right]^{2\gamma_4/(\gamma_4-1)} \quad (1)$$

where

M_s = shock speed divided by sound speed a_1 ahead of shock
P_{41} = p_4/p_1 = initial pressure ratio (>1) across diaphragm
A_{41} = a_4/a_1 = initial sound speed ratio across diaphragm
g = parameter accounting for tube cross-section area change at diaphragm
γ = specific heat ratio

Subscripts 4 and 1 denote initial states of driver and driven gases, respectively.

The effect of an area change at the diaphragm can be interpreted in terms of a constant-area shock tube having initial diaphragm pressure ratio gP_{41} and sound-speed ratio $A_{41}g^{(\gamma_4-1)/2\gamma_4}$. Appropriate values of g are given in the literature, e.g., Refs. 1 and 2; g is unity for equal driver and driven-tube areas and has a maximum value of about 2 for infinite contraction ratio.

For given initial conditions of P_{41}, A_{41}, γ_4, γ_1, and g, the solution of Eq. (1) for M_s requires an iterative procedure. Extensive graphical results therefore have been given in previous publications, usually in the form M_s vs P_{41} with A_{41}, γ_4, and γ_1 as independent parameters. A large number of curves thus are required to represent shock tube performance over a range of A_{41} values for usual combinations of γ_4 and γ_1.

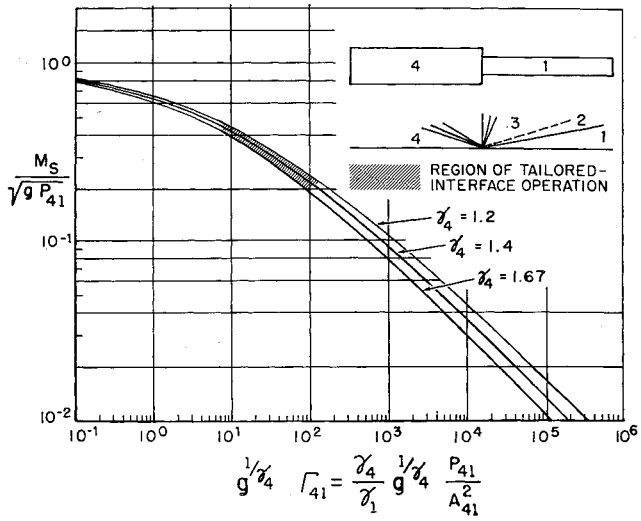

Fig. 1 Normalized shock tube performance; applicable for $M_s \geq 3$ and arbitrary γ_1

The purpose of the present note is to point out that, for M_s exceeding about 3, the approximation of neglecting 1 and $(\gamma_1 - 1)/2\gamma_1$ compared to M_s^2 enables Eq. (1) to be put into a reduced form that greatly simplifies the interpretation, graphical representation, and determination of shock-tube performance. The reduced form of Eq. (1) is

$$Y = \{1 - [(\gamma_4 - 1)/(2\gamma_4)^{1/2}]YX^{1/2}\}^{\gamma_4/(\gamma_4-1)} \quad (2)$$

where

$$Y = \left(\frac{2\gamma_1}{\gamma_1+1}\right)^{1/2}\frac{M_s}{(gP_{41})^{1/2}} \qquad X = \frac{g^{1/\gamma_4}\Gamma_{41}}{\gamma_1+1}$$

and

$$\Gamma_{41} = \gamma_4 P_{41}/\gamma_1 A_{41}^2$$

is the initial density ratio across the diaphragm. Thus the reduced equation contains only one independent parameter, γ_4, in addition to the two variables Y and X. The variable Y is the shock Mach number normalized in terms of the diaphragm pressure ratio P_{41}. The variable X is essentially the diaphragm density ratio Γ_{41} and therefore accounts for the effects of both P_{41} and A_{41}.

For practical purposes (to within a few percent accuracy), the plot of shock-tube performance from Eq. (2) can be simplified somewhat further without loss of generality by plotting $M_s/(gP_{41})^{1/2}$ vs $g^{1/\gamma_4}\Gamma_{41}$, i.e., omitting the factors in Y and X involving γ_1. The insensitivity to γ_1 (in the usual range of γ_1) is suggested by the limiting behavior of $M_s/(gP_{41})^{1/2}$ as $\Gamma_{41} \to 0$ via $A_{41} \to \infty$, and as $\Gamma_{41} \to \infty$ via $P_{41} \to \infty$. Three such plots of tube performance are shown in Fig. 1 for values of γ_4 of 1.67, 1.4, and 1.2. These curves determine M_s in convenient form for arbitrary values of P_{41}, A_{41}, γ_1, and g. It is emphasized that the curves apply only for M_s exceeding about 3.

All the basic aspects of ideal shock-tube performance are made conveniently apparent by this representation. For a given value of γ_4, the normalized performance, i.e., $M_s/(gP_{41})^{1/2}$, depends only on the diaphragm density ratio Γ_{41}. The most efficient operation for production of strong shocks, i.e., maximum M_s for given P_{41}, is at low values of Γ_{41} which are obtained with large values of the sound-speed ratio A_{41}. Some increase in performance [i.e., $M_s/(gP_{41})^{1/2}$] is obtained with decrease in γ_4, but this increase becomes small at lower values of Γ_{41}.

Received by ARS December 10, 1962. This study was done under Contract No. AF 33(657)-8860 for the Aeronautical Research Laboratory, Office of Aerospace Research, U. S. Air Force.

* Assistant Head, Aerodynamic Research Department.
† Research Mechanical Engineer.